Langmuir

Article

pubs.acs.org/Langmuir

Exceptionally Slow Movement of Gold Nanoparticles at a Solid/Liquid Interface Investigated by Scanning Transmission Electron Microscopy

Andreas Verch,[†] Marina Pfaff,[†,§] and Niels de Jonge*[,†,‡]

[†]INM – Leibniz Institute for New Materials, Campus D2 2, 66123 Saarbrücken, Germany

[‡]Department of Physics, University of Saarland, Campus A5 1, 66123 Saarbrücken, Germany

Supporting Information

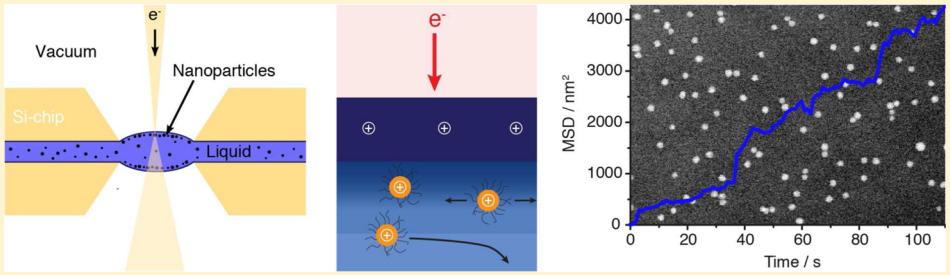

ABSTRACT: Gold nanoparticles were observed to move at a liquid/solid interface 3 orders of magnitude slower than expected for the movement in a bulk liquid by Brownian motion. The nanoscale movement was studied with scanning transmission electron microscopy (STEM) using a liquid enclosure consisting of microchips with silicon nitride windows. The experiments involved a variation of the electron dose, the coating of the nanoparticles, the surface charge of the enclosing membrane, the viscosity, and the liquid thickness. The observed slow movement was not a result of hydrodynamic hindrance near a wall but instead explained by the presence of a layer of ordered liquid exhibiting a viscosity 5 orders of magnitude larger than a bulk liquid. The increased viscosity presumably led to a dramatic slowdown of the movement. The layer was formed as a result of the surface charge of the silicon nitride windows. The exceptionally slow motion is a crucial aspect of electron microscopy of specimens in liquid, enabling a direct observation of the movement and agglomeration of nanoscale objects in liquid.

INTRODUCTION

The movement of nanoparticles in a confined liquid is commonly described by Brownian motion corrected for hydrodynamic hindrance near a wall.[1] The motion of (sub)micrometer-sized nanoparticles has been studied with ensemble averaging optical techniques, or single particle tracking techniques based on light microscopy.[2−5] Recent advances in electron microscopy in liquid made it possible to directly image nanoparticle movement at the nanoscale.[6−10] The experimental setup typically contains a thin electron transparent membrane supporting a liquid layer. Several research groups observed that nanoparticles within nanoscale proximity of a supporting membrane moved over distances of merely several tens of nanometers within the typical observation times of seconds,[6−9,11−13] many orders of magnitude slower than expected on the basis of Brownian motion.[6,9] However, the underlying mechanism is not well understood. What is the cause of slow movement of nanoparticles? Does it involve specific properties of the liquid, and the liquid interface? Is the movement slowed down as a result of hydrodynamic hindrance near a wall,[9] or are the nanoparticles adhered to the surface and move by rolling or sliding[8] over the surface?

Here, we examined the motion of gold nanoparticles under varied conditions aiming to shed light on the observed exceptionally slow motion. The liquid was enclosed between two silicon microchips supporting 50 nm thick electron transparent silicon nitride (SiN) membranes (Figure 1). The microchips were loaded into a dedicated liquid holder for transmission electron microscopes. Gold nanoparticles in liquid were detected with high contrast using STEM with an annular dark-field (ADF) detector.[14] The spatial resolution of this technique strongly depends on the liquid layer thickness.[15] The highest spatial resolution in STEM can be achieved if the feature of interest is at the top membrane, while the resolution is decreased for nanoparticles deeper in the liquid on account of beam broadening.[16]

RESULTS

To study the nanoscale movement of nanoparticles in liquid, 30 nm diameter thiolated chitosan (TCHIT) coated gold nanoparticles were dispersed in a liquid containing 80%

Received: January 14, 2015
Revised: June 3, 2015
Published: June 7, 2015

DOI: 10.1021/acs.langmuir.5b00150
Langmuir 2015, 31, 6956−6964

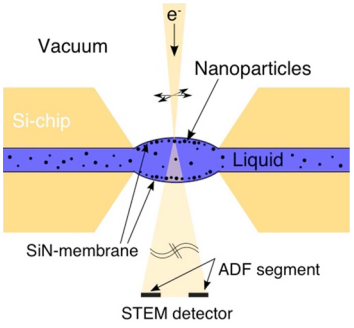

Figure 1. In liquid scanning transmission electron microscopy (STEM), the sample is enclosed between two electron transparent silicon nitride (SiN) membranes separating the liquid from the high vacuum in the microscope chamber. Contrast is obtained on nanoparticles of high atomic number (Z) by scanning a focused electron beam over the sample and recording scattered electrons using the ADF STEM detector.

(volume) glycerol, 10% water, and 10% phosphate buffered saline (PBS). These nanoparticles exhibit a positive electrical surface charge when placed in water. The usage of TCHIT coated gold nanoparticles is advantageous for the study of nanoscale movements in liquids because these nanoparticles were observed to stay within the field of view over a period of several tens of seconds. In contrast, gold nanoparticles with citrate coating (negative surface charge) did not adhere to the membrane and quickly moved out of the field of view when imaged with the electron beam. Glycerol has a higher viscosity than water and, therefore, slows down the nanoparticle movement facilitating the imaging and the tracking of the nanoparticles using electron microscopy.

STEM of Moving Nanoparticles in Liquid. Prior reports showed exceptionally slow movement of gold nanoparticles but these experiments involved an ultrathin liquid layer at an evaporating droplet[8] or below a bubble[6] known to form in a closed liquid cell without flow,[17−20] so that only thin liquid layers resided on the silicon nitride membrane windows (Figure 2a). Our first question was thus whether slow nanoparticle movement takes place in a completely filled liquid cell or whether this effect only occurs in an ultrathin liquid layer. We have tested the nanoparticle movement at the interface of such a bubble in the liquid. The bubble appeared upon continued electron beam irradiation of the specimen, as was found also in previous studies presumably by the formation of hydrogen gas.[6,8,13,18,20] Note that the formation of bubbles can be prevented by flowing the liquid in the sample chamber between the SiN windows.[10,21] Figures 2b−d show stills from a movie

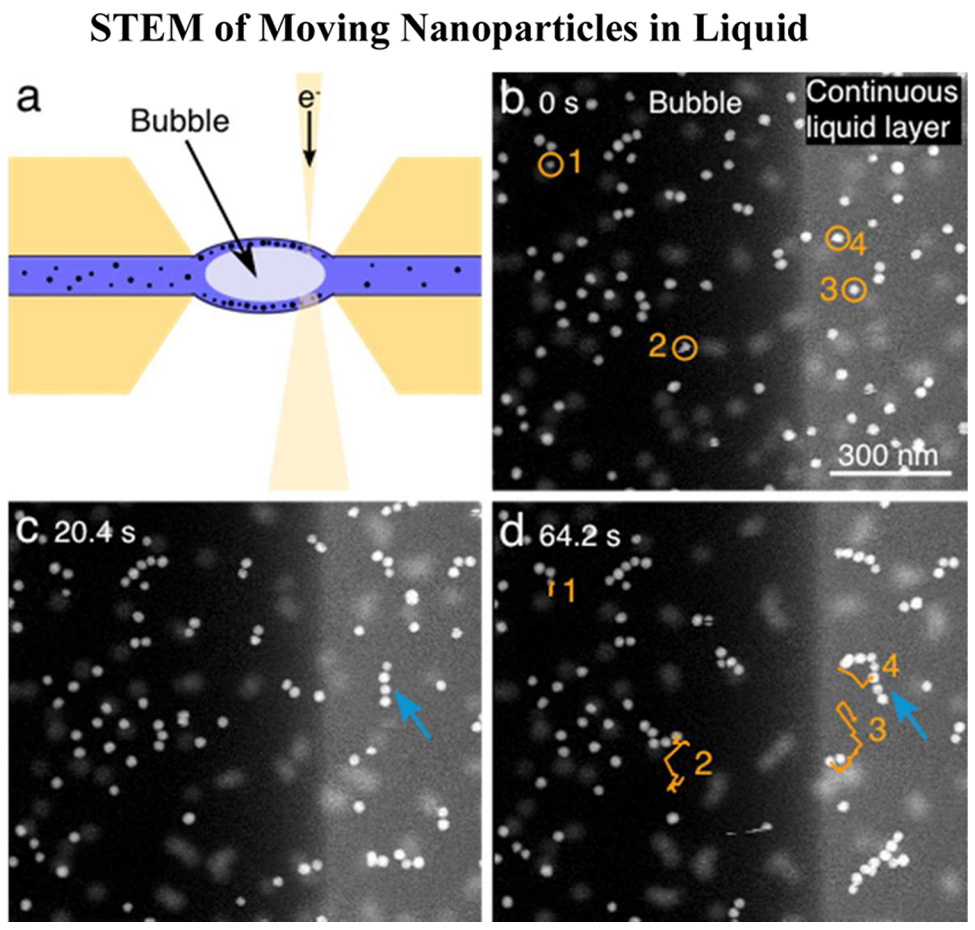

Figure 2. Liquid STEM of nanoparticles in liquid at the location of a bubble. (a) Schematic of the bubble in the liquid between the two silicon nitride windows. The effective liquid layer thickness in the bubble region was reduced compared to the region with a continuous liquid layer. (b−d) Stills from an ADF STEM time-lapse series at different time points of TCHIT coated 30 nm diameter gold nanoparticles in a solution containing 80% glycerol and 20% phosphate buffered saline (PBS). The electron dose rate was 1.1 e^{-}/sÅ^2. The images were recorded at the interface of a bubble, so that the liquid layer thickness at the left side was smaller than that at the right side. Nanoparticles deeper in liquid appear blurred. The tracks of four exemplary nanoparticles (marked in b)) are displayed in orange in (d). The blue arrows point to a chain of agglomerated nanoparticles.

DOI: 10.1021/acs.langmuir.5b00150
Langmuir 2015, 31, 6956−6964

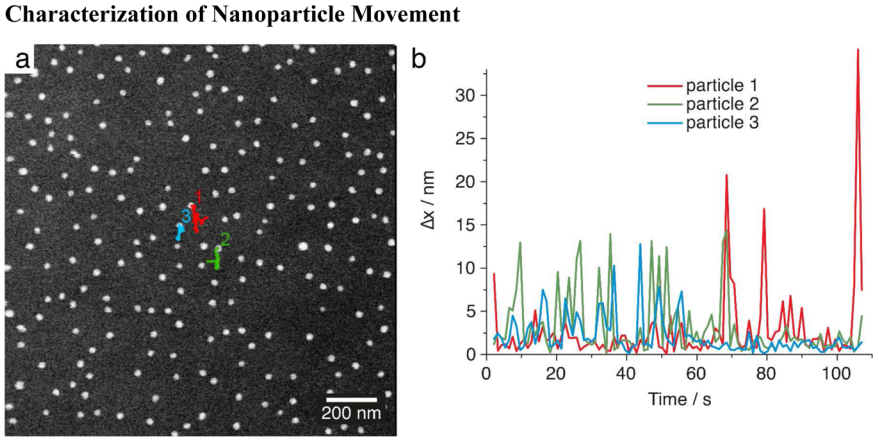

Figure 3. Nanoscale movement of TCHIT coated gold nanoparticles in liquid studied with Liquid STEM. The liquid was 80% glycerol in pure water. The electron dose rate was 1.0 $e^-/sÅ^2$. (a) ADF STEM image of gold nanoparticles in liquid at the onset of movement. The trajectories of three nanoparticles as observed in a time-lapse STEM series are indicated as colored lines. (b) Analysis of the trajectories of the three nanoparticles highlighted in (a). The step size Δx from one to the next image is plotted as a function of time.

(Supporting Information Movie S1) recorded at this interface position of the bubble using ADF STEM of the TCHIT coated gold nanoparticles in solution. The nanoparticles were initially adhered to the negatively charged supporting silicon nitride membrane. The attraction was presumably by both electrostatic and van der Waals force. Most nanoparticles started to move after a certain period of irradiation with the electron beam. The STEM electron beam was focused on the nanoparticles at the top silicon nitride membrane, while nanoparticles at the bottom appeared blurred.

The left side of the image is darker than the right side, and from the reduced background obtained with ADF STEM, it follows that less liquid was present in this region. We thus interpret the left side as a bubble. The transition area at the edge of the bubble exhibits a gradient in the gray scale indicating a gradient of the liquid layer thickness. The thickness of the liquid layer was measured via the transmitted current passing through the opening in the annular dark-field detector. The continuous liquid layer had a thickness of 0.7 μm. The vertical position of the bubble in the liquid cell is unknown, but from the fact that we observed nanoparticles moving at the top and the bottom window, we deduce that liquid resided on both membranes. It seems to be plausible that the bubble did not entirely displace the liquid, since the silicon nitride windows were hydrophilic after plasma cleaning.

The movement of the nanoparticles appeared in a random, that is, nondirectional, manner as illustrated by the tracks of four exemplary nanoparticles drawn in Figure 2d. Most nanoparticles in the fully filled region and in the transition region made steps of several tens of nanometers between frames. These steps are much slower than what is expected on the basis of Brownian motion. One would typically expect that particles of these dimensions move by distances of ~1 μm between two frames (see Discussion). Sometimes streaks were observed, indicating fast movement with a certain component parallel to the direction of the line scan. These nanoparticles disappeared from the field of view. The nanoparticles in the bubble area moved slower than the nanoparticles in the continuous liquid layer, that is, the tracks of nanoparticles #3 and #4 in Figure 2d are much longer than that of nanoparticle #1. Thus, the nanoparticles in the bubble region moved even slower than those in the continuous liquid. From this experiment, it can be concluded that slow nanoparticle movement also takes place in a liquid layer much thicker than the diameter of the nanoparticles.

Figure 2 also shows another effect that was observed regularly. Closely approaching nanoparticles often adhered, and sometimes even agglomerated into chains, as illustrated by the arrow in Figure 2c, d. The formation of one-dimensional (1D) chains of positively charged nanoparticles was also observed by Liu et al.[7] They studied the movement and self-assembly of gold nanoparticles coated with cetyltrimethylammonium ions (CTA+). They concluded that the hydrated electrons formed during imaging reduced the positive charge of the nanoparticles thus canceling the repulsive electrostatic forces between the nanoparticles. In this view, the formation of chains is attributed to electron beam induced polaron-like states that create a dipole moment with the charged polymer coating. Zhang et al. reported that the formation of 1D structures of thiol-ligand capped gold nanoparticles in aqueous solutions is mainly driven by an anisotropic dipolar interaction caused by the gold−sulfur bonding between ligand and nanoparticle.[22]

Characterization of Nanoparticle Movement. In order to characterize the nanoparticle movement in a full liquid layer (without bubble), a new liquid cell was loaded and several time-lapse series of ADF-STEM images were recorded with electron dose rates ranging from 0.2 to 4 $e^-/sÅ^2$. The chance of formation of bubbles was reduced by ultrasonication of the liquid prior to loading in order to remove dissolved gas. The sample again contained 30 nm diameter TCHIT coated gold in a liquid consisting of 80% (volume) glycerol and 20% water. The liquid thickness was 1.6 μm. Figure 3a shows an ADF STEM image of gold nanoparticles on a silicon nitride membrane. The liquid is too thick for nanoparticles at the other side of the liquid cell to be visible on account of beam broadening.[15] Most nanoparticles seem to have been immobilized on the window at the onsite of STEM. The volume of enclosed liquid within the field of view of 3.6×10^{-18} m^3 would yield a total of 2×10^2 gold nanoparticles from the applied solution. The number of nanoparticles in Figure 3a measures 215, and so the number of nanoparticles on both windows would have been 4×10^2. Considering the inaccuracy of the concentration determination, this number found on the membrane fits the expected number assuming that all nanoparticles immobilized.

DOI: 10.1021/acs.langmuir.5b00150
Langmuir 2015, 31, 6956−6964

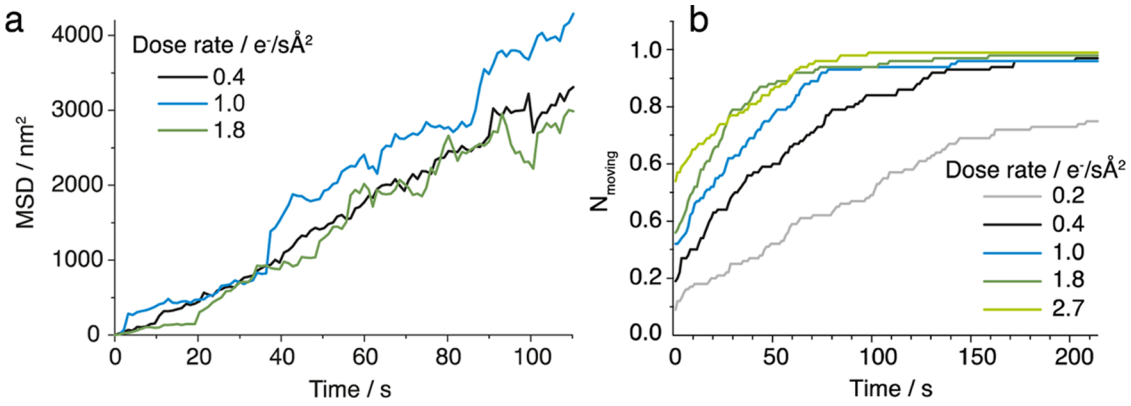

Figure 4. Influence of the electron dose rate on the particle movement. The investigated nanoparticles were TCHIT coated gold nanoparticles in a glycerol–water mixture. (a) Mean square displacement MSD as a function of the elapsed time obtained from 20 trajectories of moving nanoparticles for each electron dose rate. The curve of the dose rate of 1.0 $e^-/sÅ^2$ corresponds to the data shown in Figure 3. (b) Fraction of nanoparticles that had moved N_{moving} for different electron dose rates in liquid STEM.

As for the other sample, most nanoparticles started to move after a certain period of irradiation with the electron beam (see Movie S2). An important question is whether the nanoparticles move collectively, or rather independently. This question was addressed by analyzing the occurring step size for different particles as a function of time. A particle tracking analysis of moving gold nanoparticles was performed. Several tens of nanoparticles were considered that had moved within the analyzed time period. The criterion that a particle had moved was that it had moved by at least half its diameter. Many nanoparticles were found to move continuously after the first step, while some particles remained stationary for a period of time after a few steps of movement. Figure 3b shows the step sizes of three particles over 100 frames of ~1 s each, and it follows from the random appearing step sizes with time that the movement is random; see also Movie S2. It also appeared that there was no preferred direction of movement. Similar random movement in steps was also observed by others.[8] Note that Movies S1 and S2 do not show collective movement of the nanoparticles, neither radially nor in a horizontal direction, which was reported to occur in the presence of bubbles or at the edge of a drying patch.[6,8,9] Directed movement was sometimes observed in the present study for samples containing a bubble.

Particles moving by Brownian motion do not display a directional preference but a group of particles starting from one position randomly moves and is distributed over a volume of increasing radius with elapsing time. The mean square displacement MSD is commonly used to analyze Brownian motion or random walk and is defined as[3]

$$\mathrm{MSD} = \langle \Delta x^2(\tau) \rangle = \frac{1}{N} \sum_{i=1}^{N} (\vec{x_i}(\tau) - \vec{x_i}(0))^2 \quad (1)$$

where $\vec{x_i}(\tau)$ is the position of trajectory i after time τ, and N denotes the number of trajectories. The data of Movie S2 was analyzed and Figure 4a depicts the corresponding MSD as a function of time obtained from 20 analyzed trajectories (the curve with the dose rate of 1.0 $e^-/sÅ^2$). The MSD curve follows an approximate linear behavior, as was also observed by others,[8] and the slope amounted to 29 nm^2/s. Note that the overall movement of the gold nanoparticles differed between experiments. In some experiments the overall movement was slower than in others, while streaks were visible in a few experiment indicating fast moving nanoparticles.

Influence of the Electron Dose. Since the electron irradiation triggered the detachment of the nanoparticles thus initiating the movement, an important topic is the influence of the electron beam on the movement. Therefore, the nanoparticle displacement distribution was investigated as a function of the electron dose by imaging the same sample as was used for Movie S2 at different magnifications. The nanoparticle displacement was then analyzed with respect to the electron dose rate (current per area and time). Three curves of the MSD, representing different electron dose rates, are plotted in Figure 4a. Although there are some differences between the shapes of the curves (especially the curve for 1.0 $e^-/sÅ^2$), no correlation between the electron dose rate and the slope of the curves was found. We attribute the differences to the inaccuracy of the measurement and the statistical variation of the experimental results.

The electron dose influenced the speed at which the nanoparticles detached upon electron irradiation. The fraction of nanoparticles that had moved is plotted over the time for different electron dose rates in Figure 4b. The time until the nanoparticles detached from the membrane depended on the electron dose rate. All nanoparticles had detached at least once at the highest dose rate of 2.7 $e^-/sÅ^2$ after 100 s, but only 50% of the nanoparticles had moved for the lowest dose rate of 0.2 $e^-/sÅ^2$ after the same time interval. This observation indicates that the electron beam induced the detachment process. Since the electron dose did not influence the speed of movement, we assume that the electrostatic interactions between the nanoparticles were not notably influenced by the electron beam impact. If on the contratry, the electron beam impact would have caused, for example, strong positive charging of the nanoparticles, they would have experienced a stronger repulsion between each other with increasing dose rate, and this would have led to faster movements. The effect leading to the detachment of the nanoparticles is thus presumably that the electron beam causes secondary emission leading to the formation of a positive electrical charge in the silicon nitride membrane that repels the positively charged nanoparticles.[7] The observation that the nanoparticles detached faster with a higher electron dose is consistent with the idea of an increasing positive charge of the membrane with increasing dose.

DOI: 10.1021/acs.langmuir.5b00150
Langmuir 2015, 31, 6956–6964

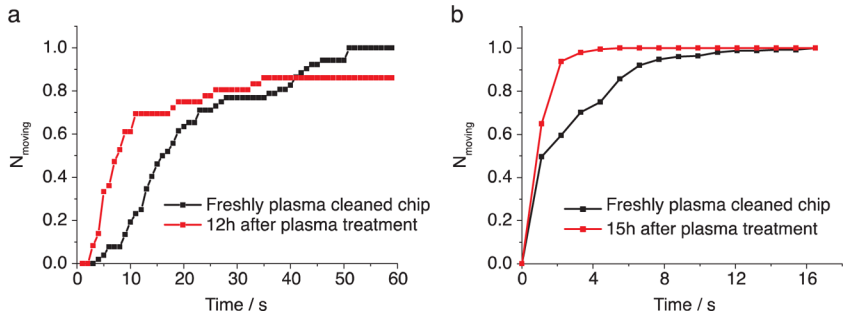

Figure 5. N_{moving} as a function of time of TCHIT coated gold nanoparticles for different experimental situations. The case of a silicon nitride membrane with high surface charge directly after plasma treatment is compared with the case of a lowered surface charge. The situation of a liquid cell filled with PBS (a) is compared with the case of 80% glycerol and 20% PBS (b).

Influence of Electrical Charge on Movement. Nanoparticle interactions are known to depend on the involved surface charges[23] (and of course many other parameters such as viscosity, radius, solvation energy, etc.), and so we studied several different configurations. To test for a possible influence of the particle charge on the movement, experiments were conducted using negatively charged citrate coated gold nanoparticles (Movie 3). The nanoparticles in this sample were not adhered to the membrane but moved freely in the liquid. A few blurred shapes appeared to move quickly upon electron beam irradiation. It can be seen that these movements exhibit much fewer small steps than in case of the TCHIT coating. Most of these nanoparticles made a few large steps and then disappeared from the field of view. We did not analyze trajectories for these nanoparticles because they consisted of a few steps only.

The possible influence of electrostatic (Debye) screening[23] was tested by comparing a liquids with and without added salt. It was expected that screening would be reduced in pure water compared to saline, possibly leading to an increased range of the repulsive force between the nanoparticles and thus larger velocities. The movements shown in Figure 2 were of a sample with 10% PBS, while the data shown in Figure 3 did not contain salt. The movements of nanoparticles at the right side in Figure 2 (Movie S1) were analyzed, and the MSD was determined for 27 trajectories. The slope amounted to 23 nm^2/s similar as the data recorded in glycerol and pure water (Figure 4 curve 1.0 $e^-/sÅ^2$) within the statistical variation of the experiment. Thus, these experiments do not show an influence of electrostatic screening on the speed of movement.

Third, the influence of the surface charge of the silicon nitride membrane was investigated. Since the nanoparticles moved in close proximity of the membrane, an influence of this surface charge was expected. The silicon nitride membrane was usually plasma cleaned shortly prior to the loading of the liquid cell. The membrane was then found to be wetting for water and thus had a high hydrophilicity. Surface charges and an increase of hydrophilicity were induced during the treatment with an Ar/O_2-plasma. This process removes organic contaminations that lower the hydrophilicity. In addition, the oxygen species present in the plasma react with the silicon nitride membrane creating polar and hydrophilic $Si-(OH)_x$ groups at the surface. For comparison with a situation with a reduced surface charge and lower hydrophilicity, another sample was made using silicon nitride membranes that were left in ambient air for 12 h after plasma cleaning. These membranes were found to be less wetting and thus less hydrophilic than in the case of a freshly plasma cleaned membrane but it was also not repelling for water. A liquid cell with these membranes was filled with 30 nm diameter TCHIT coated gold nanoparticles in liquid containing 80% (volume) glycerol, 10% water, and 10% phosphate buffered saline (PBS).

A time-lapse STEM series was recorded (Movie S4) showing significant differences from the situation of a freshly plasma cleaned silicon nitride membrane (Movie S2). Immobilized gold nanoparticles were present but the nanoparticles detached from the silicon nitride membrane much quicker upon electron beam irradiation and then moved out of the field of view with one step. It was thus not possible to analyze the trajectories. Instead, we analyzed the fraction of nanoparticles that had either moved one step larger than half their diameter or moved out of the image as a function of time. Figure 5a shows that the gold nanoparticles detached much quicker for the case of a silicon nitride membrane with reduced hydrophilicity, that is, surface charge than for the case of a freshly plasma cleaned membrane.

Influence of the Viscosity. The viscosity of the liquid is generally believed to influence the speed of Brownian motion. To test this effect, a sample was prepared exhibiting a much lower viscosity using PBS as only liquid (no glycerol). The result was a remarkable increase in the speed of movement. Figure 6 depicts an image with nanoparticles, many of which moved quickly as is apparent from the streaks. See also Movie

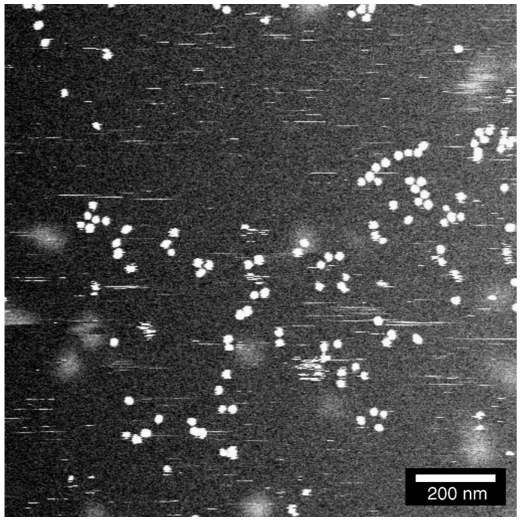

Figure 6. STEM image of TCHIT coated gold nanoparticles in a layer of PBS. The streaks indicate fast moving nanoparticles. Electron dose rate = 2.2 $e^-/sÅ^2$.

DOI: 10.1021/acs.langmuir.5b00150
Langmuir 2015, 31, 6956−6964

S5. The streaks indicate particles moving with a directional velocity component in the direction of the STEM scan and a similar speed.[10] It was not possible to follow trajectories for these nanoparticles. The nanoparticles in pure PBS also detached much more rapidly upon electron beam irradiation (Figure 5b).

DISCUSSION

Vertical Movement. In order to discuss the movement of the positively charged TCHIT coated gold nanoparticles, we will first consider vertical movement perpendicular to the silicon nitride membrane. The positively charged nanoparticles adhered to the SiN membrane with negative surface charge directly after loading (Figure 7a). In order for the nanoparticles

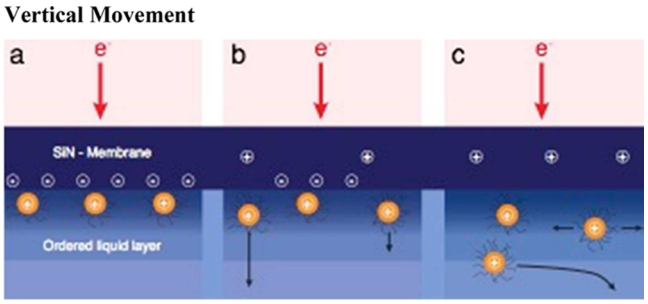

Figure 7. Model of the interaction of gold nanoparticles in liquid upon electron beam irradiation. (a) Negatively charged TCHIT coated gold nanoparticles adhered to the SiN membrane initially on account of the negative surface charge of the membrane. The first nanometers of liquid consisted of an ordered liquid layer. (b) The SiN membrane charged positively upon electron beam irradiation, so that the nanoparticles detached from the membrane. (c) Several nanoparticles moved parallel to the membrane within the ordered liquid layer at a distance in which the attractive van der Waals force was in balance with the electrostatic repulsive force. Some nanoparticles moved out of the ordered layer and started to move quickly.

to detach from the membrane, they were repelled, presumably by positive charging of the membrane as a result of the electron beam impact (Figure 7b). However, this repelling electrostatic force had only a short-range as a result of electrostatic screening in water.[23] Note that it is not possible from our data to calculate the magnitude of the electrostatic interaction because we do not know the exact charges of membrane and nanoparticles. They were attracted to the membrane by van der Waals forces expressed as[23]

$$F = -\frac{k_A a}{6d^2} \tag{2}$$

with k_A being the Hamaker constant of a value amounting to 1.5×10^{-19} J for water, a being the radius of the nanoparticle, and d being the distance between the surface of the particle and the membrane. This equation assumes that $d \ll a$. One could thus assume that the detached nanoparticles were attracted to the silicon membrane by van der Waals force and repelled by short-range electrostatic force. Solvation energy of the nanoparticles may also have played a role. The net force would be zero at a certain distance d_{zero} between the membrane and the particle, and the vertical positions of the particles would thus equilibrate at this position. The nanoparticles would then preferentially move in two small vertical regions parallel to the silicon nitride membranes (Figure 7c). In Movie S1 it can be observed that two types of objects move in the right-hand side of the image where the space between the two silicon nitride membranes is filled with liquid. Small nanoparticles appear sharply defined in-focus, and a second species appearing rather blurred. There does not seem to be a species transitioning from sharp to blurred. Thus, the data seems consistent with the presence of two layers of gold nanoparticles at the top and bottom membrane, respectively. The liquid layer is too thick in Movie S2 to see movements at the deeper positioned membrane, and here we can only observe one nanoparticle layer. Here again, the nanoparticles do not seem to move vertically, that is, going in-and-out of focus and reside at proximity of the membrane

Horizontal Movement. *Comparison of Experiments with the Theory of Brownian Motion.* The nanoparticles seem to have moved freely in horizontal direction (Movies S1 and S2), that is, parallel to the silicon nitride membrane at distance d_{zero} for a certain period of time. Note that some of the nanoparticles showed stationary periods after initial movement. Eventually, most irradiated nanoparticles moved out of the field of view (Figure 7c). The most striking observation is the extremely slow movement of the nanoparticles. In order to assess the observed particle speeds, we have considered particle motion by Brownian motion. For an observed two-dimensional (2D) motion, the mean square displacement $\langle \Delta x^2(\tau) \rangle$ is related to the diffusion coefficient D via:[3]

$$\langle \Delta x^2(\tau) \rangle = 4D\tau \tag{3}$$

Particles would thus be found in an area with radius r from their starting position after time τ:

$$r = \sqrt{\langle \Delta x^2(\tau) \rangle} = \sqrt{4D\tau} \cong \Delta\bar{x} \tag{4}$$

This radius approximately equals the average displacement of particles $\Delta\bar{x}$. Depending on the strength of the force keeping the nanoparticles in a vertical plane, the motion obtains a 2D nature. To compare the experimental results with theoretical values, the diffusion coefficient D was calculated via the Stokes–Einstein relation:[24]

$$D = \frac{k_B T}{4\pi\eta a} \tag{5}$$

where k_B is the Boltzmann constant, T is the temperature, and η is the dynamic viscosity of the liquid. The viscosity of a 80% (volume) glycerol solution in water at 22.5 °C is $\eta = 0.053$ Pa·s,[25] so that $D = 4.1 \times 10^5$ nm^2/s; see Table 1. This value is 5 orders of magnitude larger than the experimentally determined value of $D = 7$ nm^2/s, as follows from MSD = 29 nm^2/s, a

Table 1. Comparison of the Nanoparticle Movements between Liquid STEM at 200 keV, and Theoretical Values for Brownian Motion[a]

condition	$\Delta\bar{x}$ (nm)	D (nm^2/s)	η (Pa·s)
nanoparticle movement in 80% glycerol	5	7	3×10^3
theory, 80% glycerol, bulk	1.6×10^3	4.1×10^5	0.053
theory, 80% glycerol, 1 nm gap	9.8×10^2	1.6×10^5	0.053
theory ,water, bulk	1.2×10^4	2.4×10^7	8.9×10^{-4}
Theory pure glycerol	3.3×10^2	1.8×10^4	1.19

[a]The average displacement $\Delta\bar{x}$ between images of a time lapse series, the diffusion coefficient D, and the viscosity[25] η are given. The time elapsed between the recording of two STEM images was $\tau = 1.07$ s. The temperature was 22.5° C. The particle diameter was 30 nm.

DOI: 10.1021/acs.langmuir.5b00150
Langmuir 2015, 31, 6956−6964

frame time of ∼1 s, and using eqs 1 and 3. The theoretical displacement of a 30 nm diameter nanoparticles from one image to another $\Delta\bar{x}$ = 1.6 μm is almost 3 orders of magnitude larger than the observed displacements for TCHIT coated gold nanoparticle of 30 nm diameter in 80% glycerol and 20% PBS in experiments with a freshly plasma cleaned silicon nitride membrane. The diffusion constant is 2 orders of magnitude larger for pure water and indeed the speed at which gold nanoparticles detach from the silicon nitride membrane is 1 order of magnitude larger than for the case of glycerol.

Hydrodynamic Hindrance. One possible explanation for the observed exceptionally low speed is a restricted movement in proximity of the silicon nitride membrane due to hydrodynamic hindrance. Nanoparticles close to a wall are known to move differently than nanoparticles in a liquid without any borders, as described by the hydrodynamic near wall hindrance theory.[9] This effect can be taken into account by introducing a correction factor λ^{-1} based on an asymptotic solution of the Stokes equations.[1,3,26] The diffusion coefficient for movements parallel to a wall $D_{\|}$ is then

$$D_{\|} = \lambda_{\|}^{-1} D \tag{6}$$

The correction factor can be calculated with the following approximation:[1,26]

$$\lambda_{\|}^{-1} = 1 - \frac{9}{16}\left(\frac{a}{z}\right) + \frac{1}{8}\left(\frac{a}{z}\right)^3 - \frac{45}{256}\left(\frac{a}{z}\right)^4 - \frac{1}{16}\left(\frac{a}{z}\right)^5 \tag{7}$$

Here, z denotes the distance between the nanoparticle center and the wall. Even if the nanoparticle moves almost directly on the silicon nitride membrane leaving a gap of only 1 nm between nanoparticle and membrane, so that $z = a + 1$ nm, the diffusion coefficient is decreased to 39% of its bulk value. For larger distances, the correction factor increases and approaches one. The proximity effect is thus not an explanation for the observed slow movement, and the correction factor can be neglected considering the variation in our data.

Phase Separation. A further possibility is that the solution had separated out in its two components, whereby the glycerol was localized at the interface with the silicon nitride membrane. In this case, the viscosity in the liquid layer directly at the membrane would have been that of glycerol. Although the diffusion would then have been a factor 23 lower than for the bulk liquid, this difference is still far from sufficient to explain the slow movement of the gold nanoparticles (Table 1).

Ordered Liquid Layer at Surface. Neither wall hindrance of Brownian motion nor phase separation of the liquid explain the small measured diffusion constant. The question is thus: what else can be the cause of this slow motion? A possible explanation for extremely slow nanoparticle motion is a large increase of the viscosity of the liquid in nanoscale proximity of the silicon nitride membrane. Water at a hydrophilic surface was reported to form an interface layer extending up to 5 nm from the surface with a viscosity of 6 orders of magnitude larger than that of bulk water;[27] such layers can be studied using an atomic force microscopy tip.[28] The properties of the interfacial layer are governed by a high degree of order of the water molecules bound to the surface by hydrogen bonds.[23] The ordering effect could possibly also occur for the liquid used here containing glycerol and water. As discussed above, the nanoparticles presumably moved at a distance d_{zero} from the silicon nitride membrane. Possibly this distance was within this interfacial layer of ordered liquid with largely increased viscosity (Figure 7c). The formation of an ordered liquid layer is known to be promoted by the surface charge of the solid surface.[27] Indeed, the effect of slow movement occurred for a freshly plasma cleaned membrane only, while in the case of a more hydrophobic surface preventing the formation of an ordered layer, the nanoparticles moved away from the field of view quickly (Figure 5). Based on the measured MSD ≈ 25 nm^2/s, it follows that the viscosity in 80% glycerol has been $\eta \approx 3 \times 10^3$ Pa•s, 5 orders of magnitude larger than that for bulk liquid. Also for samples containing 100% water (no glycerol), nanoparticles detached slower from freshly plasma cleaned membranes than from those, which were exposed to air for a couple of hours, indicating slower movement at the hydrophilic surface.

Obviously, the model presented here is oversimplified and the interactions taking place at the solid/liquid interface are much more complex. We do not rule out that different effects cause the slow motion. An alternative explanation could be that the nanoparticles merely rolled or shifted over freshly plasma cleaned silicon nitride membrane, due to strong TCHIT−gold membrane attraction.[8] The electron beam lowered the adhesion between nanoparticle and membrane but the particles did not gain enough energy to leave the interface. Observations made by others at the edge of a drying droplet revealed a much smaller diffusion constant for 15 nm diameter nanoparticles, but in this case the water layer may have been so thin that the nanoparticles were pinned to the surface.[8] At first sight, this finding appears contradictory because smaller nanoparticles would move faster. However, the nanoparticles may have been more embedded in this highly viscous layer than was the case in our experiment. The literature agrees on the observation of slow movement, but the reported speeds range a few orders of magnitude, and this range does not seem to be explained by the range in sizes of the used nanoparticles.[6−9,11−13] However, it is difficult to compare these data since measurements of the liquid thickness are mostly absent. The model of an interface layer of ordered liquid seems plausible at least for nanoparticles in a liquid of a thickness much larger than their diameter, and this model is consistent with our experimental data.

■ CONCLUSIONS

Liquid STEM can be used to study the movement of nanoparticles in a liquid in the presence of an electron beam. Samples containing gold nanoparticles with different coatings in water or in a water-glycerol mixture were investigated via the recording of time-lapse movies. It was found that nanoparticles with a positive surface charge initially adhered to the silicon nitride membrane, detached upon electron beam irradiation, presumably as a result of positive charging of the membrane upon electron beam impact. Nanoparticles with a negative surface charge were not observed in close proximity to the membrane. The usage of water instead of glycerol increased the speed of detachment by an order of magnitude. The positively charged nanoparticles then moved in horizontal direction with random steps and directions at a preferred distance from the silicon nitride membrane, for a liquid containing 80% glycerol on a freshly plasma cleaned membrane. It was verified that this effect occurred in a fully filled liquid cell, and not just at the edge of a bubble or drying droplet as was reported previously.[6,8] The movement was 3 orders of magnitude slower than that predicted from the theory of Brownian motion. The exceptionally slow movement could not be explained by a correction for hydrodynamic hindrance near a wall[1,26] or phase separation

DOI: 10.1021/acs.langmuir.5b00150
Langmuir 2015, 31, 6956−6964

of the liquid. Instead, it seems plausible that a layer of highly ordered liquid[27] was present on the silicon nitride membrane, increasing the viscosity by 5 orders of magnitude.

The exceptionally slow moment movement of nanoparticles in liquid is a crucial aspect of electron microscopy of specimens in liquid, since obviously nanoparticles would not be observable with nanoscale resolution if their movement would follow Brownian motion for bulk liquids. It is thus possible to directly image movement of nanoparticles in liquid at the nanoscale within time frames of seconds. The investigated effects could have an impact on different applications in the field of nanofluidics, where nanoparticles are transported through narrow channels and are in close proximity to surrounding walls. It would possibly open a new option in structural biology to view biomolecules with TEM or STEM in liquid layer with a viscosity of 10^3 Pa·s. Furthermore, the highly reduced velocities close to the liquid−solid interface may enable exciting new studies directly viewing the agglomeration of nanoparticles on surfaces, and for self-assembly processes.

EXPERIMENTAL SECTION

Nanoparticles. For the liquid STEM experiments we used 30 nm diameter gold nanoparticles coated with TCHIT and a positive zeta potential from Nanopartz Inc. (Loveland, CO). The original concentration of the nanoparticle solution was increased by centrifugation at 4500*g* for 30 min and removal of 2/5 of the excess liquid. For the first experiment (with a bubble in the liquid cell), 1 μL of the concentrate was mixed with 1 μL of PBS and 8 μL of glycerol, resulting in a nanoparticle concentration of 4.5×10^{10} NP/μL. Phosphate buffered saline (PBS) was added to increase the conductivity of the liquid in some experiments. For most of the experiments, 1 μL of the concentrate was mixed with 8 μL of glycerol and 1 μL of deionized water (HPLC grade).

For a comparison experiment, negatively charged citrate stabilized 30 nm gold nanoparticles from British Biocell International (Cardiff, U.K.) were used. The concentration was increased. From the color of the liquid, it was estimated that the concentration was about a factor of 10 lower than that of the sample with TCHIT coated nanoparticles.

Liquid STEM. To image the nanoparticles in liquid, we used a liquid flow TEM Holder with the corresponding silicon microchips (Protochips Inc., Raleigh, NC).[16,21] These microchips support a 50 nm-thick electron transparent silicon nitride window with a size of 50×400 μm^2. Spacers on one of the chips should ensure a constant and defined distance of the two chips when they are pressed together via two O-rings in the holder. Microchips with a spacer height of either 500 nm or 2 μm were used for the presented experiments. The two Si chips were cleaned in acetone and ethanol for 2 min each prior to the assembly of the liquid cell. Subsequently, the chips were made hydrophilic by plasma cleaning them for 5 min. The loading procedure started by placing the first (smallest) microchip chip into the slot of the holder. Next, a small droplet (0.2 μL) of the nanoparticle solution was pipetted onto the chip. The liquid cell was then closed by placing the second (larger) microchip within about 10 s, thus avoiding drying of the droplet. The liquid flow capability of the holder was not used for the experiments described here. To ensure that there was no leak in the liquid cell, the windows were checked with a binocular, and the time needed to evacuate the load lock of the microscope was monitored.

The liquid STEM experiments were carried out using a transmission electron microscope (JEM-ARM 200F, JEOL, Tokyo, Japan) equipped with a cold field emission gun and a STEM probe corrector (CEOS GmbH, Heidelberg, Germany). The electron energy was 200 keV. The annular dark-field (ADF) detector was used with a camera length of 8 cm, resulting in a detector opening semiangle of 35 mrad. Image series were acquired with a script in the image acquisition software (Digital Micrograph, Gatan Inc., Pleasanton, CA). The beam current (measured via the small fluorescent screen) was approximately 99 pA. A pixel dwell time of 1 μs and an image size of 512×512 pixels were used, so that the acquisition time between two consecutive recordings amounted to 1.07 s. The pixel sizes ranged between 1.4 and 4 nm, depending on the magnification.

Determination of the Liquid Thickness. The liquid thickness in the liquid cell for each experiment was determined via a measuring the current transmitted through the sample and passing through the opening angle of the annular dark field detector on the phosphor screen in the microscope. This type of measurement was found previously to be precise within about 30% for water thicknesses between 1 and 15 μm neglecting the silicon nitride windows.[15] Since thinner liquid layers were used in some of the experiments here, a modified method was used in which the windows were taken into account. The fraction of the current density measured on the screen with and without sample inserted I_{screen}/I_0 equals:[14,15]

$$\frac{I_{screen}}{I_0} \cong \exp\left\{-\left(\frac{t_{sin}}{l_{sin}} + \frac{t_{liquid}}{l_{liquid}}\right)\right\} \quad (8)$$

with t_{SiN} and t_{liquid} being the thicknesses of the two silicon nitride membranes and the liquid, respectively. The thicknesses for both windows was 100 nm in total. The mean free path length l for scattering into the detector with opening semiangle β = 35 mrad amounts to l_{SiN} = 0.79 μm for amorphous silicon nitride with a composition of Si_3N_4 and a density of 2.6 g/cm^3. We approximated the liquid as 100% glycerol, so that l_{liquid} = 2.6 μm. For water, the value is l_{liquid} = 3.0 μm. The method was calibrated using a test sample consisting of a layer of pure water enclosed between two silicon nitride membranes and with gold nanoparticles on the outside of both windows. This window was tilted and the vertical distance between the gold nanoparticles was determined via the parallax equation to amount to 1.1 μm. The transmitted current was measured to be $I_{screen}/I_0 = 0.66$ in the middle of the liquid cell. It followed from eq 8 that the liquid thickness was 0.88 μm, which matches the thickness measured from tilting with 30%. This test was repeated for another five samples and found to be precise within 30%.

Analysis of Particle Tracks. The positions of nanoparticles in STEM time series were tracked using the ImageJ plugin MTrackJ.[29] The particles were assigned to the different trajectories manually in each frame. Trajectories were stopped when particles disappeared or aggregated with other nanoparticles. For further data analysis, lists containing information about the trajectories, such as particle positions, velocity, displacement, and so forth, for each image were generated within the plugin. In some time lapse series, collective movement caused by stage drift was identified. Sample stage drift was apparent from a uniform movement of all objects shortly after having moved the stage to this position. The drift vanished after a several seconds. The data used for Movies S1 and S2 were aligned prior to the particle tracking using the StackReg ImageJ plugin. This plugin minimized the mean square differences in the intensity between the reference and the current image.

ASSOCIATED CONTENT

Supporting Information

Movie S1: Time series of ADF STEM images recorded of 30 nm diameter gold nanoparticles in a layer of 80% glycerol and 20% saline. The movie was recorded at the location of bubble. The speed of the movie was increased by a factor of 4 with respect to the original data. Pixel size = 2.3 nm, electron dose rate = 1.1 e$^-$/sÅ^2. The data set was corrected for stage drift. Movie S2: Time-lapse STEM movie of 30 nm diameter TCHIT coated gold nanoparticles in a layer of 80% glycerol and 20% pure water. The speed of the movie was increased by a factor of 4 with respect to the original data. Pixel size = 3.0 nm, electron dose rate = 1.0 e$^-$/sÅ^2. The data set was corrected for stage drift. Movie S3: Time series of ADF STEM images recorded of 30 nm diameter citrate coated gold nanoparticles in a layer of 80% glycerol and 20% pure water. The speed of the movie was

DOI: 10.1021/acs.langmuir.5b00150
Langmuir 2015, 31, 6956−6964

increased by a factor of 4 with respect to the original data. Pixel size = 4.7 nm, electron dose rate = 0.6 $e^-/sÅ^2$. Movie S4: Time-lapse STEM movie of 30 nm diameter TCHIT coated gold nanoparticles in a layer of 80% glycerol and 20% pure water. The silicon nitride was kept in ambient air for 12 h after plasma cleaning to reduce the surface charge. The speed of the movie was increased by a factor of 4 with respect to the original data. Pixel size = 3.7 nm, electron dose rate = 0.9 $e^-/sÅ^2$. Note that the data shows stage drift in the first few seconds. Movie S5: Time-lapse STEM movie of 30 nm diameter TCHIT coated gold nanoparticles in a layer of pure water. The speed of the movie was increased by a factor of 4 with respect to the original data. Pixel size = 2.5 nm, electron dose rate = 2.2 $e^-/sÅ^2$. The Supporting Information is available free of charge on the ACS Publications website at DOI: 10.1021/acs.langmuir.5b00150.

AUTHOR INFORMATION

Corresponding Author

*Telephone +49-681-9300313. E-mail: niels.dejonge@leibniz-inm.de.

Present Address

[§]M.P.: Bosch, Stuttgart, Germany.

Notes

The authors declare no competing financial interest.

ACKNOWLEDGMENTS

The microchips and the specimen holder were provided by Protochips Inc., Raleigh, NC. We thank Eduard Arzt for his support through INM.

REFERENCES

(1) Lin, B.; Yu, J.; Rice, S. A. Direct measurements of constrained Brownian motion of an isolated sphere between two walls. *Phys. Rev. E* **2000**, *62*, 3909−3919.

(2) Bevan, M. A.; Prieve, D. C. Hindered diffusion of colloidal particles very near to a wall: Revisited. *J. Chem. Phys.* **2000**, *113*, 1228−1236.

(3) Kihm, K. D.; Banerjee, A.; Choi, C. K.; Takagi, T. Near-wall hindered Brownian diffusion of nanoparticles examined by three-dimensional ratiometric total internal reflection fluorescence microscopy (3-D R-TIRFM). *Exp. Fluids* **2004**, *37*, 811−824.

(4) He, K.; Babaye Khorasani, F.; Retterer, S. T.; Thomas, D. K.; Conrad, J. C.; Krishnamoorti, R. Diffusive dynamics of nanoparticles in arrays of nanoposts. *ACS Nano* **2013**, *7*, 5122−5130.

(5) Hassan, P. A.; Rana, S.; Verma, G. Making sense of brownian motion: Colloid characterization by dynamic light scattering. *Langmuir* **2015**, *31*, 3−12.

(6) Ring, E. A.; de Jonge, N. Video-frequency scanning transmission electron microscopy of moving gold nanoparticles in liquid. *Micron* **2012**, *43*, 1078−1084.

(7) Liu, Y.; Lin, X.-M.; Sun, Y.; Rajh, T. In situ visualization of self-assembly of charged gold nanoparticles. *J. Am. Chem. Soc.* **2013**, *135*, 3764−3767.

(8) Zheng, H.; Claridge, S. A.; Minor, A. M.; Alivisatos, A. P.; Dahmen, U. Nanocrystal diffusion in a liquid thin film observed by in situ transmission electron microscopy. *Nano Lett.* **2009**, *9*, 2460−2465.

(9) White, E. R.; Mecklenburg, M.; Shevitski, B.; Singer, S. B.; Regan, B. C. Charged nanoparticle dynamics in water induced by scanning transmission electron microscopy. *Langmuir* **2012**, *28*, 3695−3698.

(10) Ring, E. A.; de Jonge, N. Microfluidic system for transmission electron microscopy. *Microsc. Microanal.* **2010**, *16*, 622−629.

(11) Chen, X.; Wen, J. In situ wet-cell TEM observation of gold nanoparticle motion in an aqueous solution. *Nanoscale Res. Lett.* **2012**, *7*, 598.

(12) Chen, Q.; Smith, J. M.; Park, J.; Kim, K.; Ho, D.; Rasool, H. I.; Zettl, A.; Alivisatos, A. P. 3D motion of DNA-Au nanoconjugates in graphene liquid cell electron microscopy. *Nano Lett.* **2013**, *13*, 4556−4561.

(13) Proetto, M. T.; Rush, A. M.; Chien, M. P.; Abellan Baeza, P.; Patterson, J. P.; Thompson, M. P.; Olson, N. H.; Moore, C. E.; Rheingold, A. L.; Andolina, C.; Millstone, J.; Howell, S. B.; Browning, N. D.; Evans, J. E.; Gianneschi, N. C. Dynamics of soft nanomaterials captured by transmission electron microscopy in liquid water. *J. Am. Chem. Soc.* **2014**, *136*, 1162−1165.

(14) Reimer, L.; Kohl, H. *Transmission electron microscopy: physics of image formation*; Springer: New York, 2008.

(15) de Jonge, N.; Poirier-Demers, N.; Demers, H.; Peckys, D. B.; Drouin, D. Nanometer-resolution electron microscopy through micrometers-thick water layers. *Ultramicroscopy* **2010**, *110*, 1114−1119.

(16) Schuh, T.; de Jonge, N. Liquid scanning transmission electron microscopy: Nanoscale imaging in micrometers-thick liquids. *C. R. Phys.* **2014**, *15*, 214−223.

(17) Abellan, P.; Woehl, T. J.; Parent, L. R.; Browning, N. D.; Evans, J. E.; Arslan, I. Factors influencing quantitative liquid (scanning) transmission electron microscopy. *Chem. Commun.* **2014**, *50*, 4873−4880.

(18) Peckys, D. B.; Veith, G. M.; Joy, D. C.; de Jonge, N. Nanoscale imaging of whole cells using a liquid enclosure and a scanning transmission electron microscope. *PLoS One* **2009**, *4*, e8214.

(19) Woehl, T. J.; Jungjohann, K. L.; Evans, J. E.; Arslan, I.; Ristenpart, W. D.; Browning, N. D. Experimental procedures to mitigate electron beam induced artifacts during in situ fluid imaging of nanomaterials. *Ultramicroscopy* **2013**, *127*, 53−63.

(20) Grogan, J. M.; Schneider, N. M.; Ross, F. M.; Bau, H. H. Bubble and pattern formation in liquid induced by an electron beam. *Nano Lett.* **2014**, *14*, 359−64.

(21) de Jonge, N.; Pfaff, M.; Peckys, D. B. Practical aspects of transmission electron microscopy in liquid. *Adv. Imaging Electron Phys.* **2014**, *186*, 1−37.

(22) Zhang, H.; Fung, K.-H.; Hartmann, J.; Chan, C. T.; Wang, D. Controlled chainlike agglomeration of charged gold nanoparticles via a deliberate interaction balance. *J. Phys. Chem. C* **2008**, *112*, 16830−16839.

(23) Israelachvili, J. N. *Intermolecular and surface forces*, 3rd ed.; Academic Press: Waltham, MA, 2011.

(24) Einstein, A. Über die von der molekularkinetischen Theorie der Wärme geforderte Bewegung von in ruhenden Flüssigkeiten suspendierten Teilchen. *Ann. Phys.* **1905**, *322*, 549−560.

(25) Sheely, M. Glycerol viscosity tables. *Ind. Eng. Chem.* **1932**, *24*, 1060−1064.

(26) Goldman, A. J.; Cox, R. G.; Brenner, H. Slow viscous motion of a sphere parallel to a plane wall—I Motion through a quiescent fluid. *Chem. Eng. Sci.* **1967**, *22*, 637−651.

(27) Kim, H. I.; Kushmerick, J. G.; Houston, J. E.; Bunker, B. C. Viscous "interphase" water adjacent to oligo(ehtylene glycol)-terminated monolayers. *Langmuir* **2003**, *19*, 9271−9275.

(28) Guriyanova, S.; Mairanovsky, V. G.; Bonaccurso, E. Super-viscosity and electroviscous effects at an electrode/aqueous electrolyte interface: an atomic force microscope study. *J. Colloid Interface Sci.* **2011**, *360*, 800−804.

(29) Meijering, E.; Dzyubachyk, O.; Smal, I. Methods for cell and particle tracking. *Methods Enzymol.* **2012**, *504*, 183−200.

DOI: 10.1021/acs.langmuir.5b00150
Langmuir 2015, 31, 6956−6964